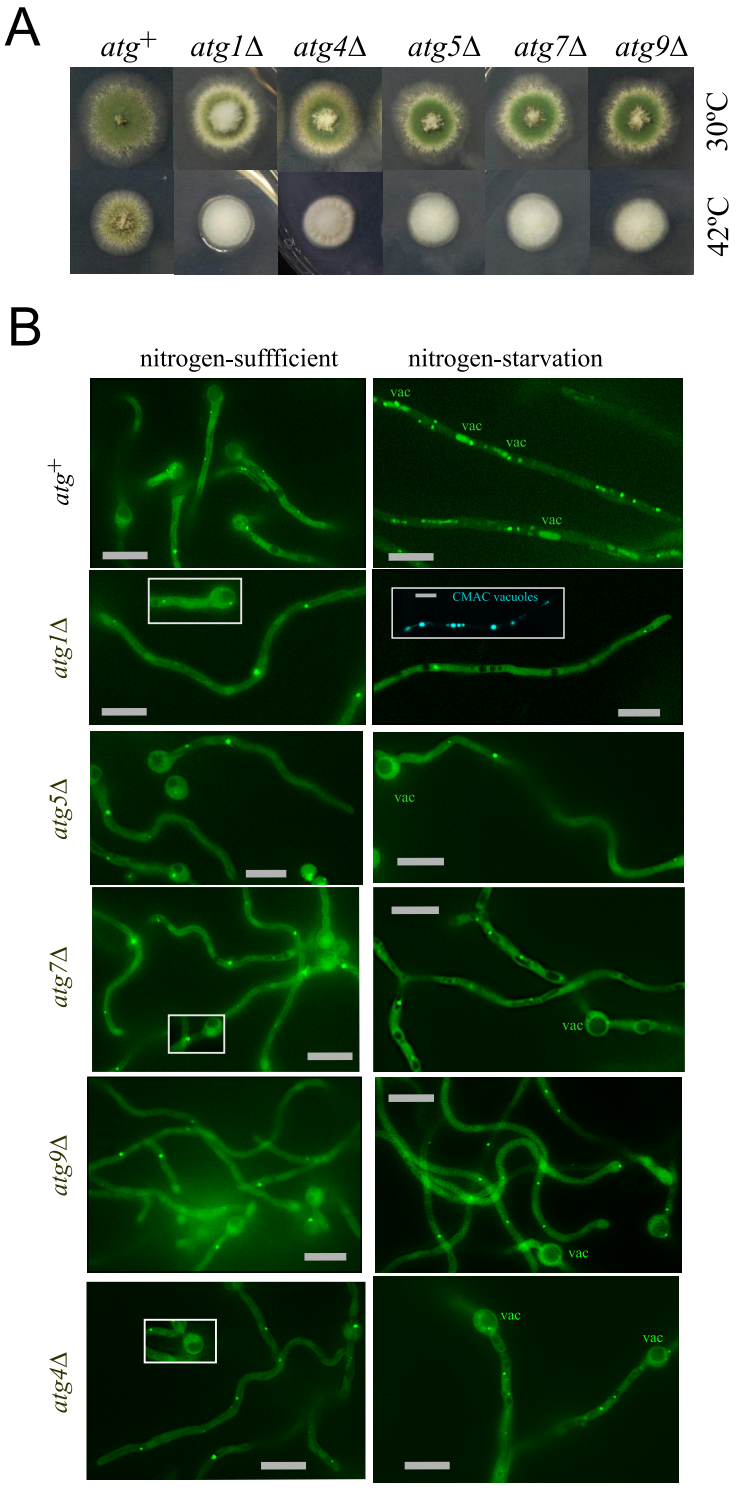

Figure S1. Phenotypic features of autophagy mutants. (**A**) *atg*Δ alleles can be scored in the progeny of crosses because at 42ºC they result in slightly impaired growth and are unable to produce conidiospores (colored asexual spores, green in the wild-type) on the surface of the colony (**B**) GFP-Atg8 localization in autophagy-deficient mutants. Left column images, in nitrogen-sufficient conditions GFP-Atg8 localizes to punctate cytosolic structures in the wild type and in the indicated *atg*Δ mutants, with the vacuoles devoid of GFP fluorescence. After a 4 h incubation (right column) in autophagy-inducing conditions, GFP-Atg8 localizes to the vacuoles (indicated with vac) and PAS puncta in the wild type. In contrast, vacuoles of *atg*Δ mutants are devoid of GFP fluorescence. In the case of *atg1*Δ, a CMAC image of the mutant is included to confirm the positions of vacuoles. For all panels, bars indicate 10 μm. In some panels, insets containing vacuoles devoid of fluorescence have been included.

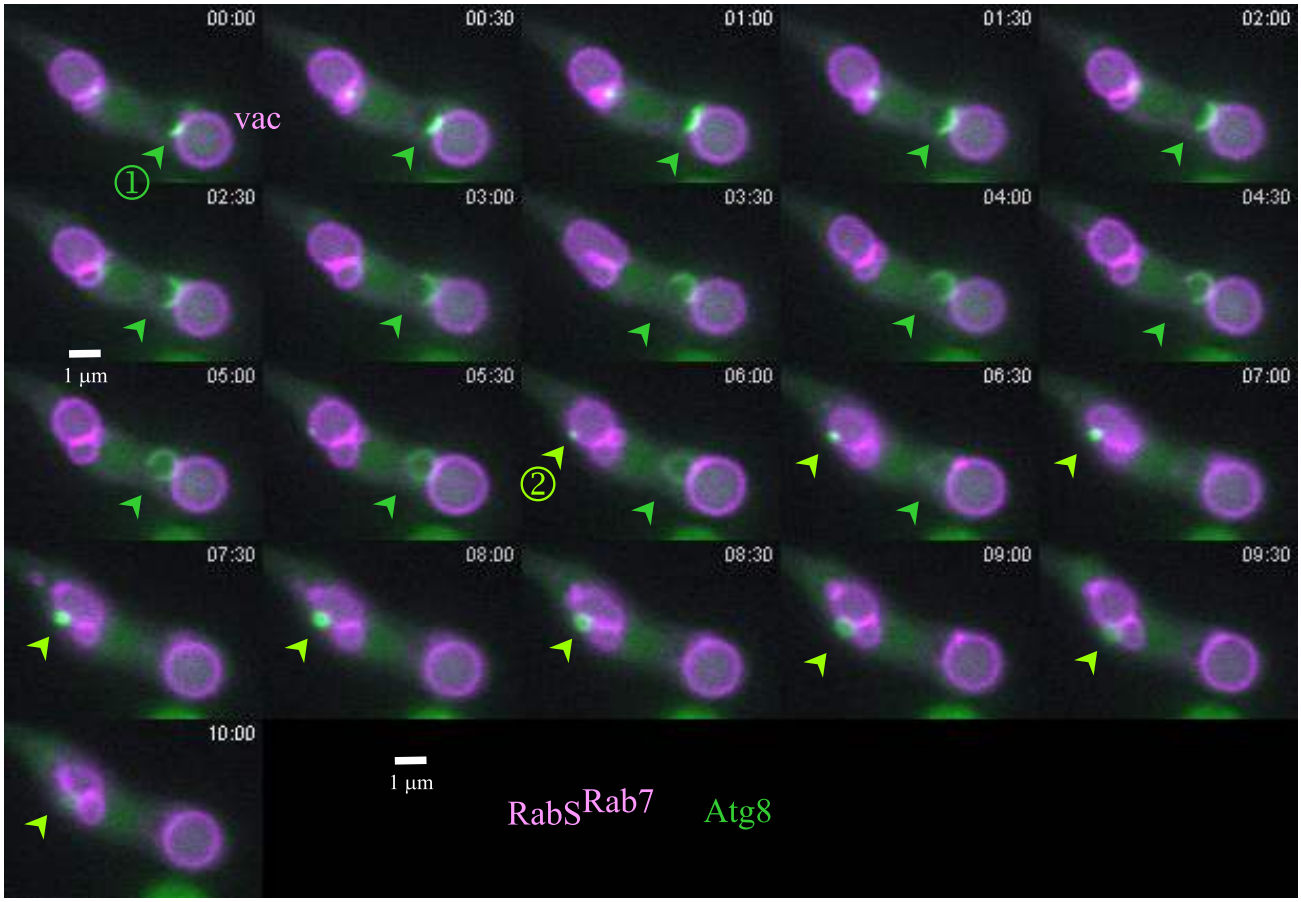

Figure S2. Still images of a time-series showing two examples of autophagosome cycles (autophagic structures are labeled with GFP-Atg8) photographed in a cell expressing mCherry-RabS^{RAB7} to visualize the vacuolar membranes. Autophagosome #1 undergoes a complete cycle. Time is in min:sec.

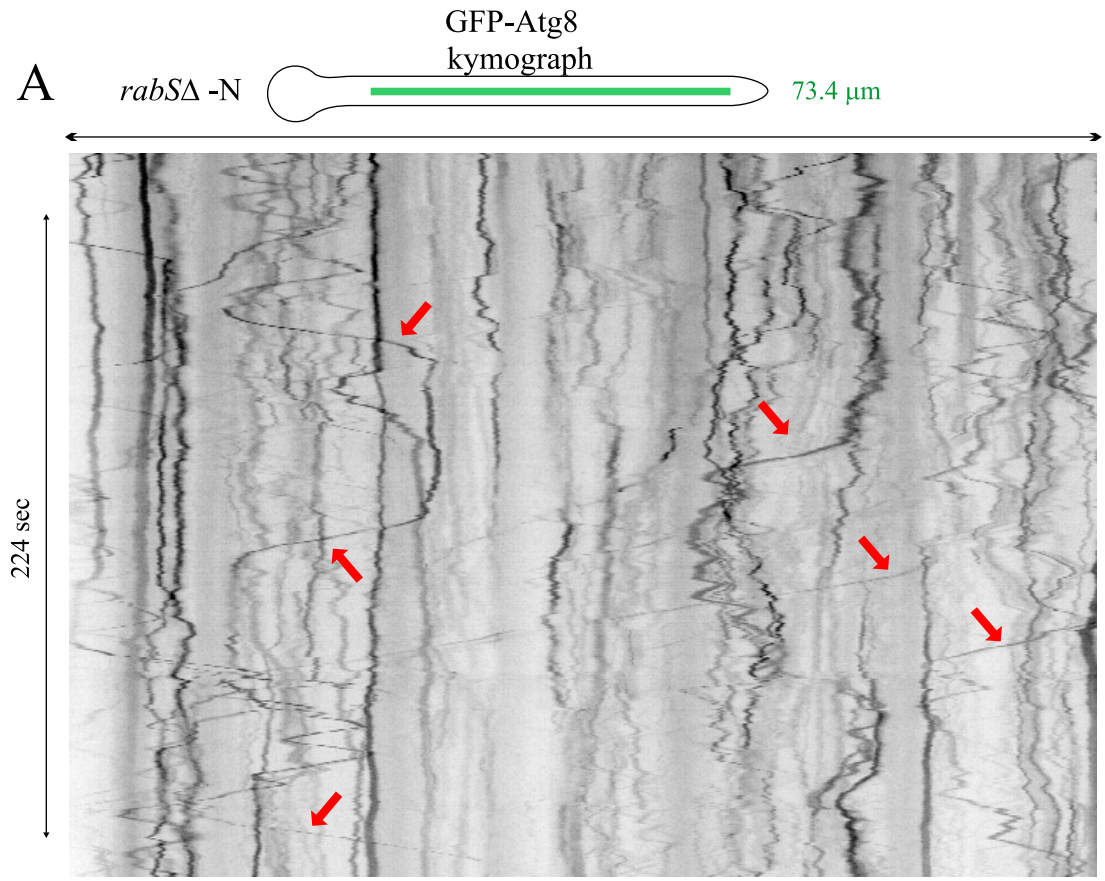

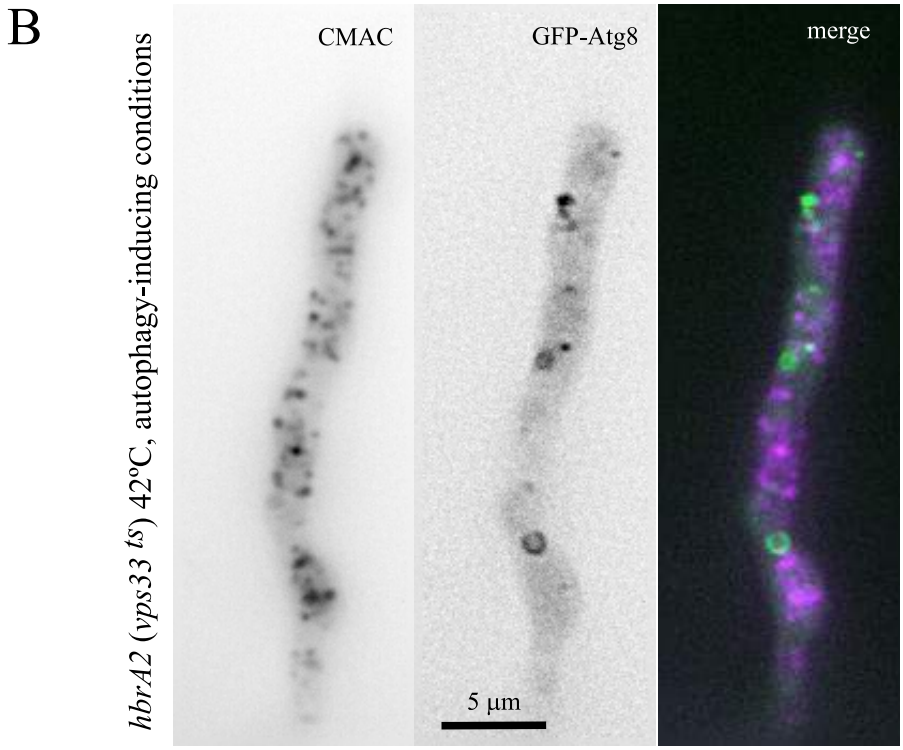

Figure S3. Autophagosomal structures formed in the absence of endovacuolar fusion machinery components (**A**) Kymograph obtained from a time-lapse sequence (504 frames, ~2.25 frames/sec) showing the motility of GFP-Atg8 structures in a *rabS*Δ cell that had been cultured under autophagy-inducing conditions. *rabS*Δ prevents homotypic fusion of late endosomes and vacuoles. Note that, in addition to vertical lines (static GFP-Atg8 structures), there are structures showing long-distance motility (diagonal lines indicated with red arrows) (see **Fig. 3F**). (**B**) Mutant *hbrA2* cells expressing GFP-Atg8 to label autophagosomes were shifted to autophagy-inducing conditions at 42ºC, loaded with CMAC to stain vacuoles (which are numerous and small due to the lack of HbrA2/Vps33 activity) and imaged in the CMAC and GFP channels. Note the presence of a closed autophagosome and an expanding phagophore, in spite of the inactivation of HbrA2/Vps33.

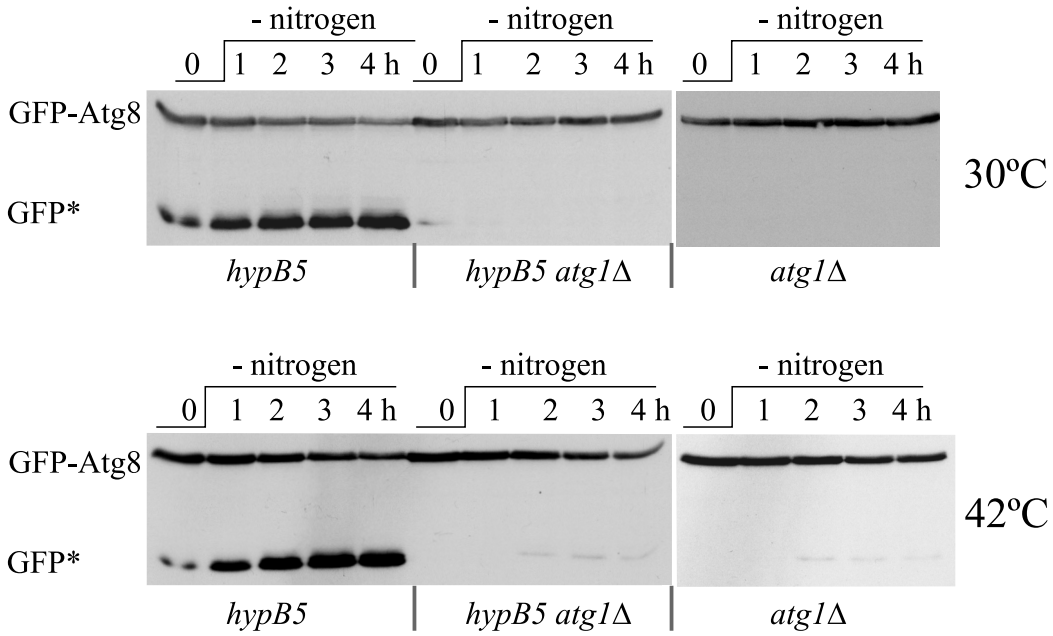

Figure S4. GFP-Atg8 proteolysis assays in the indicated mutant strains, showing that proteolysis that takes place normally in *hypB5*^{ts} cells incubated in autophagy conditions at 30ºC or 42ºC is prevented by an *atg1*Δ mutation, and thus it is autophagy dependent.

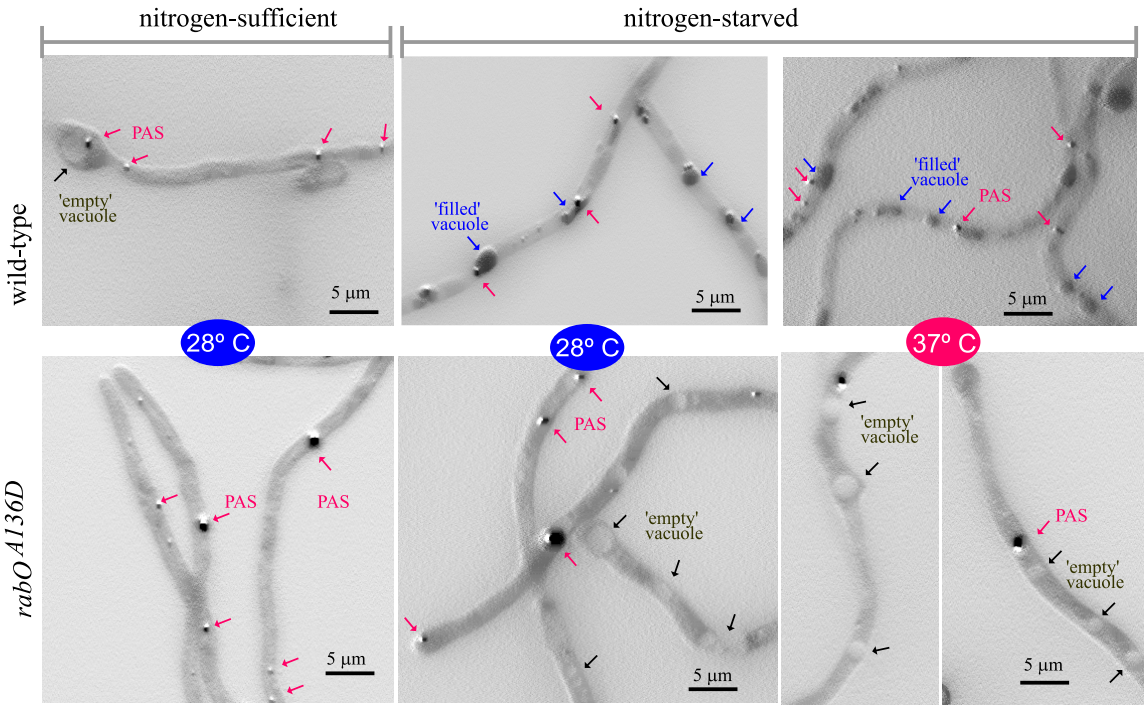

Figure S5. *rabO*^{A136D} cells are unable to deliver GFP-Atg8 to the vacuole under nitrogen starvation conditions. In wild type or mutant cells cultured with ammonium at 28ºC, GFP-Atg8 is not delivered to the vacuoles, which appear 'empty' against the cytosolic fluorescence. In contrast, in wild type cells starved for nitrogen for 4 h, GFP-Atg8 is efficiently delivered to the vacuole regardless of the incubation temperature. This nitrogen starvation-dependent delivery is completely prevented by *rabO*^{A136D} at either 28ºC or 37ºC (permissive and restrictive temperature for growth, respectively). Black arrows, empty vacuoles; red arrows, Atg8 puncta; Navy blue arrows, 'filled' vacuoles. Images are maximal intensity projections of z-stacks, processed with the 'unsharp' filter of Metamorph.

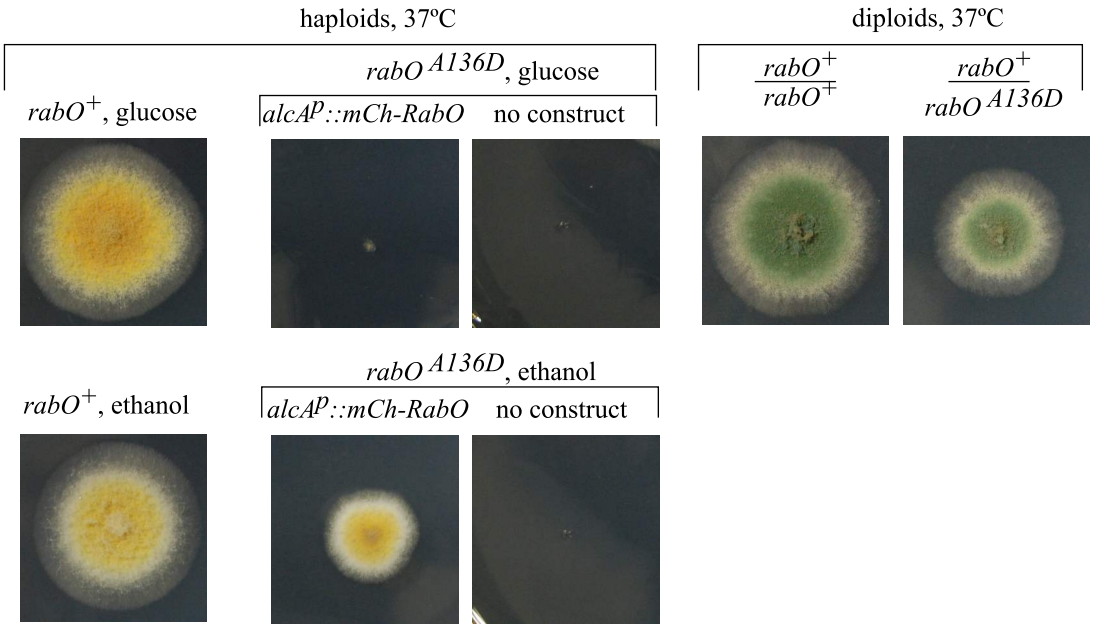

Figure S6. mCherry-RabO^{RAB1} rescued the 37ºC lethality phenotype resulting from the *rabO^{A136D}* mutation, indicating that the fusion protein is functional. Left (yellow conidiospore strains): growth of a *rabO^{A136D}* strain is rescued by the *alcA^{p}::mCherry-RabO* transgene on ethanol (inducing *alcA^{p}* conditions) but not on glucose (repressing *alcA^{p}* conditions). Green conidiospore colonies on the right correspond to a diploid strain showing that *rabO^{A136D}* is codominant to the wild type allele, such that a heterozygous diploid grows less than a homozygous wild type diploid strain. Thus, the transgene rescues *rabO^{A136D}* to essentially the same extent as the wild type allele.

Table S1. Strains used in this work

MAD0005	*wild-type*	our collection
MAD1739	*pyrG89; pyroA4 nkuAΔ::bar*	H.N.Arst
MAD2133	*pabaA1; wA4; pyroA4[pyroA*-alcA^{p}::(vps27-FYVE)$_2$::gfp] inoB2*	Abenza et al, 2010
MAD2194	*wA4 rabBΔ::pyroA^{Af}; pyroA4[pyroA*-alcA^{p}::(vps27-FYVE)$_2$::gfp] nkuAΔ::bar*	Abenza et al, 2010
MAD2743	*yA2; pyroA4; pantoB100*	our collection
MAD3230	*wA4; synA^{p}::synA::gfp::pyrG^{Af}; inoB2*	Abenza et al, 2010
MAD2819	*wA3; hypA1; synA^{p}::synA::gfp::pyrG^{Af}*	This study
MAD3263	*yA2 pabaA1; hbrA2 (vps33^{ts})*	Geoft Turner
MAD3313	*pyrg89, pyroA4 nkuAΔ::bar; atg1Δ::pyrG^{Af}*	This study
MAD3317	*wA2; pyroA4[pyroA*-rabO^{P}::gfp-rabO]; pantoB100*	This study
MAD3323	*hypB5 pabaA1 biA1; synA^{p}::synA::gfp::pyrG^{Af}*	This study
MAD3474	*yA2; pyroA4[pyroA*-gpdA^{mini}::gfp::atg8]; pantoB100*	This study
MAD3476	*pyroA4[pyroA*-gpdA^{mini}::gfp::atg8]; atg1Δ::pyrG^{Af}; pyrG89?*	This study
MAD3522	*pabaA1; rabO^{A136D}::pyrG^{Af}; pyrG89?*	This study
MAD3656	*yA2 hypB5; pyroA4[pyroA*-gpdA^{mini}::gfp::atg8]; nkuAΔ::bar?*	This study
MAD3670	*rabO^{A136D}::pyrG^{Af}; pyroA4[pyroA*-gpdA^{mini}::gfp::atg8] nkuAΔ::bar?; pyrG89?*	This study
MAD3685	*pabaA1; wA3*	H.N.Arst
MAD3692	*yA2 hypA1; pyroA4[pyroA*-gpdA^{mini}::gfp::atg8]*	This study
MAD3720	*yA2; pyroA4[pyroA*-gpdA^{mini}::gfp::atg8]; rabSΔ::pyro^{Af}; nkuAΔ::bar?*	This study
MAD3721	*wA4 rabBΔ::pyro^{Af}; pyroA4[pyroA*-gpdA^{mini}::gfp::atg8] nkuAΔ::bar?*	This study
MAD3727	*pyrG89; sedV^{R258G}::pyrG^{Af}; pyroA4 nkuAΔ::bar*	This study
MAD3737	*pabaA1; pyroA4[pyroA*-gpdA^{mini}::gfp::atg8]; pantoB100 hbrA2 (vps33^{ts})*	This study
MAD3739	*pyrG89; pyroA4 nkuAΔ::bar; atg7Δ::pyrG^{Af}*	This study
MAD3760	*yA2; pyroA4[pyroA*-gpdA^{mini}::gfp::atg8]; sltA59; vps27Δ::pyrG^{Af} pantoB100; pyrG89?*	This study
MAD3761	*yA2; pyroA4[pyroA*-gpdA^{mini}::gfp::atg8]; sltA59*	This study
MAD3762	*yA2; vps32Δ::pyrG^{Af}; pyroA4[pyroA*-gpdA^{mini}::gfp::atg8]; sltA54; pyrG89?*	This study
MAD3763	*yA2; pyroA4[pyroA*-gpdA^{mini}::gfp::atg8]; sltA54*	This study
MAD3764	*yA2; sedV^{R258G}::pyrG^{Af}; pyroA4[pyroA*-gpdA^{mini}::gfp::atg8] nkuAΔ::bar?; pyrG89?*	This study
MAD3808	*pyroA4[pyroA*-gpdA^{mini}::gfp::atg8]; atg7Δ::pyrG^{Af}; pyrg89?; nkuAΔ::bar?*	This study
MAD3900	*pabaA1; pyroA4[pyroA*-gpdA^{mini}::gfp::atg8]; copA1*	This study
MAD3902	*pyroA4[pyroA*-gpdA^{mini}::gfp::atg8]; pyrG^{Af}::niiA::vps4; pyrG89?; nkuAΔ::bar?*	This study
MAD3904	*vps41Δ::pyrG^{Af}; pyroA4[pyroA*-gpdA^{mini}::gfp::atg8] nkuAΔ::bar?; pyrG89?*	This study
MAD3927	*wA4; pyroA4[pyroA*-gpdA^{mini}::gfp::atg8]; hho::mcherry::pyroA^{Af}*	This study
MAD3929	*tlg2Δ::pyrG^{Af} pyroA4[pyroA*-gpdA^{mini}::gfp::atg8]; pantoB100; pyrG89?; nkuAΔ::bar?*	This study
MAD3960	*yA2 pabaA1; argB2[argB*-alcA^{p}::mcherry::rabS]; pyroA4[pyroA*-gpdA^{mini}::gfp::atg8]*	This study
MAD4043	*pyrG89; atg9Δ::pyrG^{Af}; pyroA4 nkuAΔ::bar*	This study
MAD4083	*yA2 pabaA1; pyroA4[pyroA*-gpdA^{mini}::gfp::atg8]; rabCΔ::pyrG^{Af}; pyrG89?*	This study
MAD4108	*pyrG89; pyroA4 nkuAΔ::bar; atg5Δ::pyrG^{Af}*	This study
MAD4111	*atg9Δ::pyrG^{Af}; pyroA4[pyroA*-gpdA^{mini}::gfp::atg8] nkuAΔ::bar?; pyrG89?*	This study
MAD4200	*pyroA4[pyroA*-gpdA^{mini}::gfp::atg8]; atg5Δ::pyrG^{Af}; pyrG89?; nkuAΔ::bar?*	This study
MAD4207	*yA2; argB2[argB*- alcA^{P}-cherry-rabO]; pyroA4[pyroA*-gpdA^{mini}::gfp::atg8] nkuAΔ::bar?*	This study

MAD4287	*sed5^{R258G}::pyrG^{Af} synA^{p}::synA::gfp::pyrG^{Af}; nkuAΔ::bar?*	This study
MAD4308	*pabaA1; rabO^{A136D}::pyrG^{Af}; synA^{p}::synA::gfp::pyrG^{Af} ; pyrG89?*	This study
MAD4423	*argB2[argB*-alcA^{p}::mcherry-rabA]; pyroA4[pyroA*-gpdA^{mini}::gfp::atg8]; rab7Δ::pyro^{Af}; nkuAΔ::bar?*	This study
MAD4426	*yA2 pabaA; rabO^{A136D}::pyrG^{Af}; argB2[argB*-alcA^{p}::mcherry::rab7]; pyroA4[pyroA*-gpda^{mini}::gfp::atg8]*	This study
MAD4438	*hypB5; pyroA4[pyroA*- gpdA^{mini}::gfp::atg8]; atg1Δ::pyrG^{Af}; pantoB100; nkuAΔ::bar?; pyrG89?*	This study
MAD4449	*synA^{p}::synA::gfp::pyrG^{Af}; copA1*	This study
MAD4446	*yA2; rabO^{A136D}::pyrG^{Af}; argB2[argB*-alcA^{p}::mcherry-rabO]; pyroA4 nkuAΔ::bar?*	This Study
MAD4451	*pyrG89; atg4Δ::pyrG^{Af}; pyroA4 nkuAΔ::bar*	This Study
MAD4472	*atg9::gfp::pyrG^{Af}; pyroA4[pyroA*- gpdA^{mini}::mcherry::atg8] nkuAΔ::bar?; pyrG89?*	This study
MAD4456	*yA2; pyroA4[pyroA*-gpdA^{mini}::gfp::atg8]; AN0834/sec63::mrfp::pyrG^{Af}; pyrG89?; nkuAΔ::bar?*	This study
MAD4488	*yA2; AN7311/trs85::gfp::pyrG^{Af}; pyroA4[pyroA*- gpdA^{mini}::mcherry::atg8]; pantoB100*	This study
MAD4490	*pyroA4[pyroA*-gpda^{mini}::gfp::atg8]; atg4Δ::pyrG^{Af}; nkuAΔ::bar?; pantoB100; pyrG89?*	This study
MAD4494	*rabO^{A136D}::pyrG^{Af} atg9::gfp::pyrG^{Af}; pyroA4[pyroA*-gpda^{mini}::gfp::atg8] nkuAΔ::bar?; pyrG89?*	This study

Movie S1. 3D reconstruction of a z-stack showing hyphae cultured under nitrogen-sufficient conditions. The cells express GFP-Atg8 to label the PAS and mCherry-histone H1 to label the nuclei. They have been stained with CMAC (blue) to label the lumina of vacuoles.

Movie S2. A general view of a hyphal tip cell expressing GFP-Atg8 that had been transferred from nitrogen-sufficient to nitrogen-starved conditions at the 'zero' time point indicated by the timer (in min:sec). Frames (in inverted contrast) correspond to fluorescence in the GFP channel. The number of punctate structures increases during the first 30–60 min, and a burst of autophagosomes is clearly visible after 60 min. At later time points, GFP fluorescence gradually appears in the vacuoles. Note that although the time resolution of this movie (1 frame every 2 min) is insufficient to visualize complete autophagosome cycles, the different intermediates of autophagosome biogenesis are noticeable, particularly between the 60 min and 150 min time points.

Movie S3. This movie illustrates the late steps of autophagy. A cell expressing GFP-Atg8 and mCherry-$RabS^{RAB7}$ to label the vacuolar membranes, incubated for 4 h in autophagy-inducing conditions. Note that the GFP fluorescence of the vacuolar lumina decays with time; at the same time, autophagosomes recur in association with the vacuoles. The timer is in min.

Movie S4. A wild-type hyphal tip cell expressing GFP-Atg8 was photographed every 5 sec in the GFP channel. The cell had been cultured under nitrogen-starved conditions to induce autophagy. The different intermediates during the biogenesis of numerous autophagosomes from punctate structures are visible over a background of faintly fluorescent vacuoles. Time in min:sec.

Movie S5. Complete autophagosome cycles (GFP-Atg8) filmed with a time resolution of 1 frame every 5 sec. Structures that eventually give rise to autophagosomes are marked with an arrow in a single frame. The positions of faintly fluorescent vacuoles are indicated in the first frame. Timer is in min:sec.

Movie S6. *rabBΔ* cells showing autophagosome cycles labeled with the PtdIns3P-binding probe $FYVE_2$-GFP. Time is in min:sec.

Movie S7. Multiple autophagosome cycles, visualized with GFP-Atg8, in $hypA1^{ts}$ cells incubated at 37ºC in autophagy-inducing conditions. Note the conspicuous swelling of the tips due to major impairment in secretion. Time is in min:secs.

Movie S8. Autophagosome cycles, visualized with GFP-Atg8, in *hypB5*^{ts} cells incubated at 37ºC in autophagy-inducing conditions. Note the conspicuous swelling, resulting from major impairment in secretion, of the only tip shown. Time is in min:secs.

Movie S9. Autophagosome cycles, visualized with GFP-Atg8, in a *sedV*^{R258G} cell incubated at 37ºC in autophagy-inducing conditions. Note the conspicuous swelling, resulting from major impairment in secretion, of the only tip shown. Time is in min:secs.

Movie S10. Time-series of images acquired in the Nomarski channel of two *rabO*^{A136D} tips at 28ºC. Tips show relatively normal apical extension rates (0.42 µm/min, top; 0.37 µm/min, bottom) indicating that secretion is not severely compromised. Time is in min:sec.

Movie S11. z-series stacks of images (z pass = 0.3 µm) taken in the red and green channels, and of its corresponding merge, showing eight different examples of ER 'omegasome-like' structures (ER labeled with AN0834/Sec63-mRFP) associated to GFP-Atg8 autophagic structures.